Contents

List of Figures

List of Tables

1 The W boson

"Potentielle citation sans aucun rapport avec le sujet"

— Personne inconnue, *contexte à déterminer*

1.1 The motivation for the W mass measurement

Being one of the cornerstones of the Standard Model (SM), the W boson is tightly connected to the other parameters of the theory. In the leading order of the perturbation theory the W mass depends only on the electroweak parameters [1]:

$$M_W = \sqrt{\frac{\pi\alpha}{\sqrt{2}G_F}}\frac{1}{\sin\theta_W}, \tag{1.1}$$

where G_F stands for the Fermi constant. The factor $\sqrt{\frac{\pi\alpha}{\sqrt{2}G_F}} \approx 40$ GeV sets the lower bound for the possible W mass. Higher order corrections enter the equation in the following way:

$$M_W = \sqrt{\frac{\pi\alpha}{\sqrt{2}G_F}}\frac{1}{\sin\theta_W}\frac{1}{1+\Delta r}, \tag{1.2}$$

where Δr contains the sum of all possible radiative corrections and depends also on other parameters of the SM, first of all on top quark and Higgs boson masses. The correction term is also sensitive to possible Beyond Standard Model (BSM) effects. As it was mentioned in Chapter 1 the mass of the W boson is one of the input parameters of the SM, so the predictions of the theory directly depend on how precisely we know the value of the boson mass. On the other hand, we can theoretically constrain the value of the W boson mass assuming the already known values of the other SM parameters. Fig. 12 demonstrates that the uncertainty of the theoretical estimate for the W boson mass is about two times

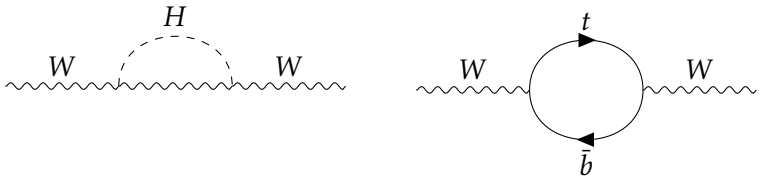

Figure 11: Next-to-leading order diagrams for W boson propagator containing contributions from heavy quarks and the Higgs boson.

lower than that of the best available experimental measurement. This motivates the effort for a more precise experimental measurement in order to test the consistency of the SM. Should the improved measurement reveal the inconsistency of the Standard Model - it would also allow to reveal viable BSM theories.

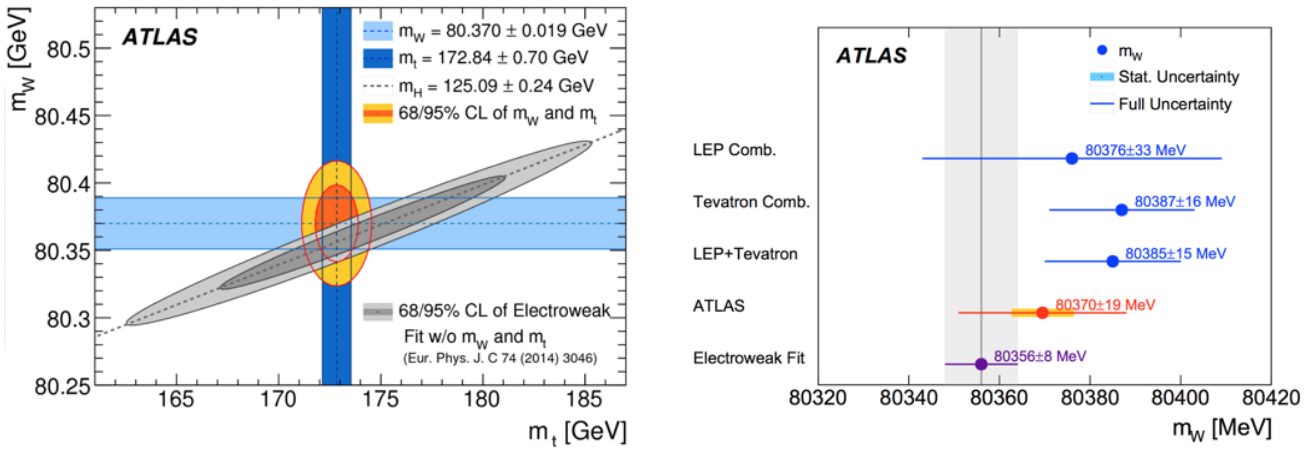

(a) W mass constraint

(b) W mass measurements

Figure 12: W mass measurements and predictions

1.2 Massive boson production at hadron colliders

Hadron colliders provide a fruitful environment for the production and study of massive electroweak bosons - all of them were discovered at hadron colliders. Hadron colliders allow to achieve much higher centre-of-mass collision energy and luminosity comparing to their lepton counterparts. At the same time precision measurements at hadron colliers demand much deeper theoretical understanding of different aspects of the SM.

The main theoretical complication of the proton-proton colliders lies in the fact that in contrary to leptons, protons are complex objects. This raises the following problems:

- A proton-proton collision is in general case a many-body problem. The absence of a consistent theory for the QCD vacuum does not allow to describe the initial state of the proton constituents in a consistent way.
- The initial energy of the whole proton is well known, but we don't know how this energy is distributed between the proton constituents.
- We know that the proton consists of three valence quarks that have non-zero expectation value and interact through gluons. In the course of these interactions all flavours of quarks (called sea quarks) are appearing off-shell. The contribution of these sea quarks to the scattering cross-section must also be taken in account.

In order to attack these problems and get accurate predictions for the proton-proton collisions it is necessary to take into account the asymptotic freedom that QCD demonstrates at short distances or high energies. At a certain energy scale of the momentum Q, transferred during the collision, we can assume that the interacting parts of the proton are asymptotically free and neglect the interaction with the rest of the proton. This is called *the factorization theorem*. The factorization occurs only if the transferred momentum $Q \gg \Lambda_{QCD}$ is large, and that is why these processes are called "hard". The physical conditions of the hard processes allow to use the perturbative QCD formalism, since at large energy scale the strong coupling constant α_s becomes small. Processes with lower energy scale of the transferred momentum are called "soft" and do not allow to use the perturbative QCD formalism. As it was mentioned in Section 1, a lot of things in the low-energy non-perturbative sector of the QCD are still unclear.

The on-shell production of massive vector bosons occurs during the hard processes, however, precise measurements at hadron colliders require understanding of both hard and soft QCD regimes. It is common that the hard scattering of the proton constituents is accompanied by a soft scattering of the remaining proton parts. This forms what is called *underlying event* and also must be taken into account.

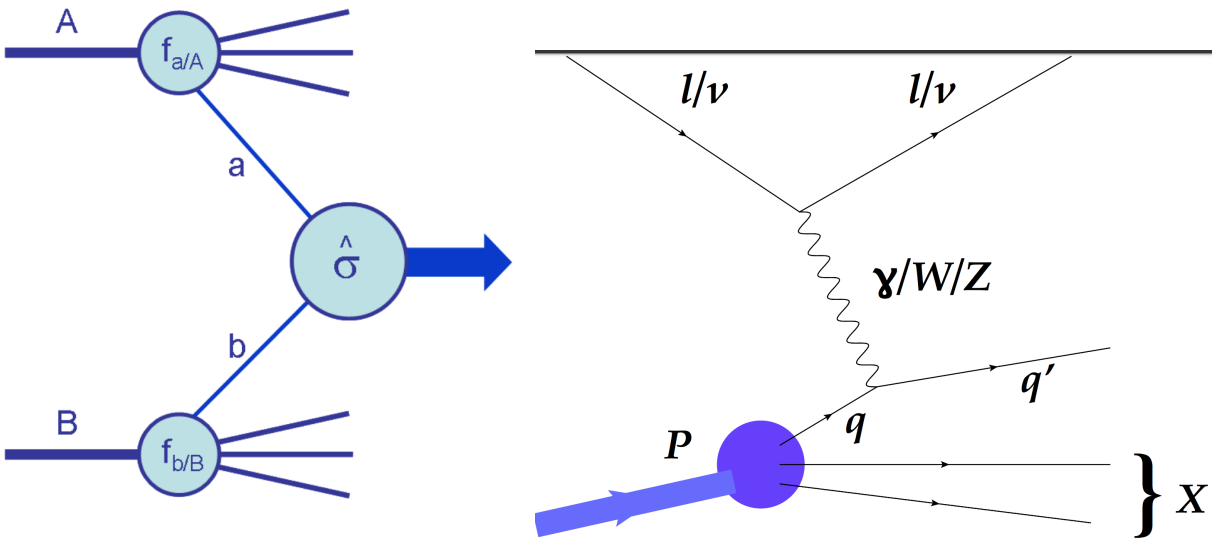

(a) Hard scattering diagram **(b)** DIS diagram

Figure 13: Examples of hard QCD scatterings.

1.2.1 Deep Inelastic scattering

In order to better illustrate the factorization approach let us first consider the lepton-hadron process called the Deep Inelastic Scattering (DIS). Historically it was the first experimental evidence for the complex structure of the proton and still serves an indispensable tool for the proton structure study.

Let's try to write a matrix element for a DIS process $e + A \to e + X$, exchanging a virtual photon with momentum q^μ:

$$|M|^2_{DIS} = 4\pi M_N \frac{\alpha}{q^4} L_{\mu\nu} W^{\mu\nu}_{hadron}, \tag{1.3}$$

where $L_{\mu\nu}$ is the transverse lepton tensor, $q^\mu L_{\mu\nu} = q^\nu L_{\mu\nu} = 0$. The hadronic tensor $W_{\mu\nu}$ along with its normalization factor $4\pi M_N$ is unknown, but we can write it down in general form introducing longitudinal and transverse parts[1] [3]:

$$W_{\mu\nu} = F_1(x, Q^2)\left(-g_{\mu\nu} + \frac{q_\mu q_\nu}{q^2}\right) + F_2(x, Q^2)\frac{\left(p_\mu - q_\mu p \cdot q/q^2\right)\left(p_\nu - q_\nu p \cdot q/q^2\right)}{p \cdot q}, \tag{1.4}$$

with p_μ being the momentum of the hadron A, Q^2 is the exchange momentum, $x = \frac{Q^2}{2p \cdot q}$ and the form-factor functions $F_1(x, Q^2)$, $F_2(x, Q^2)$ are unknown.

The cross-section of the DIS process can be measured experimentally, leaving the possibility to study the form-factor functions. It turned out that these functions do not depend (at least in the first approximation) on Q^2 [**dis**]. Further experiments have revealed that they form-factors depend only on the ratio x, as it was predicted before [4]. This type of behaviour was called the Bjorken scaling.

These results have led to the idea of partons - point-like constituents of the proton [5]. Keeping in mind the idea of factorization we can assume the lepton only interacts with one of the partons. Then we can express the hadronic tensor $W_{\mu\nu}$ as a sum of all available partons:

$$W_{\mu\nu}(q_\mu, p_\nu) = \sum_a \int_x^1 \frac{d\xi}{\xi} f_{a/A}(\xi, \mu) H^a_{\mu\nu}(q_\mu, p_\nu, \mu, \alpha_s(\mu)) + NLO. \tag{1.5}$$

The functions $H^a_{\mu\nu}(q_\mu, p_\nu, \mu, \alpha_s(\mu))$ are called the hard scattering structure functions and only depend on parton type a, but not on hadron type A. These functions describe the high-energy behaviour and can be calculated in the framework of perturbative QCD. At the same time $f_{a/A}(\xi, \mu)$ is called Parton Density Function (PDF) and has a physical meaning of finding a parton of type a (gluon, u-quark, d-quark etc) in a hadron of type A (proton, neutron, meson) carrying the fraction of ξ of the hadron's momentum. These PDFs contain information on the momentum distribution of quarks and gluons within the hadron. This corresponds to the non-perturbative sector of the QCD which is beyond the reach of theoretical methods available so far. Note that they do not directly depend on the momentum Q^2, but only on the energy scale μ.

The DGLAP equations show that once the PDFs are known at a certain energy scale μ they can be perturbatively extrapolated to a different energy scale [6], [7], [8], [9]. This means that the PDFs are universal - they can be measured experimentally at certain conditions in the course of the DIS (or any other) process and then used for numerical calculations of any other process (e.g. Drell-Yan (DY) process) at different conditions. Such a measurement allows a workaround - we may not be able to solve the many-body problem and perform non-perturbative calculations starting from the first principles, yet we still get a theoretical prediction with a good precision. Currently there exist a number

[1] Given example assumes only electromagnetic interaction. For the more general electroweak case the tensor structure is more complicated and there are more than two scalar structure functions [2].

of different groups working on the PDF parametrizations and fits, constantly improving the fits using the data coming from hadron colliders. Using different PDF sets may give different results and also helps to estimate the systematic uncertainties implied by the PDFs.

Historically the DIS experiments at HERA electron-proton collider have allowed to perform proton PDFs measurements with a good level of precision in the x region up to $x \backsim 10^{-4}$ at high Q^2. The HERA experiments operated until 2008, paving the path for precision predictions for the Drell-Yan process. Currently there are prospects for new experiments like Large Hadron Electron Collider (LHeC) that would involve DIS and further improve the PDF precision [10].

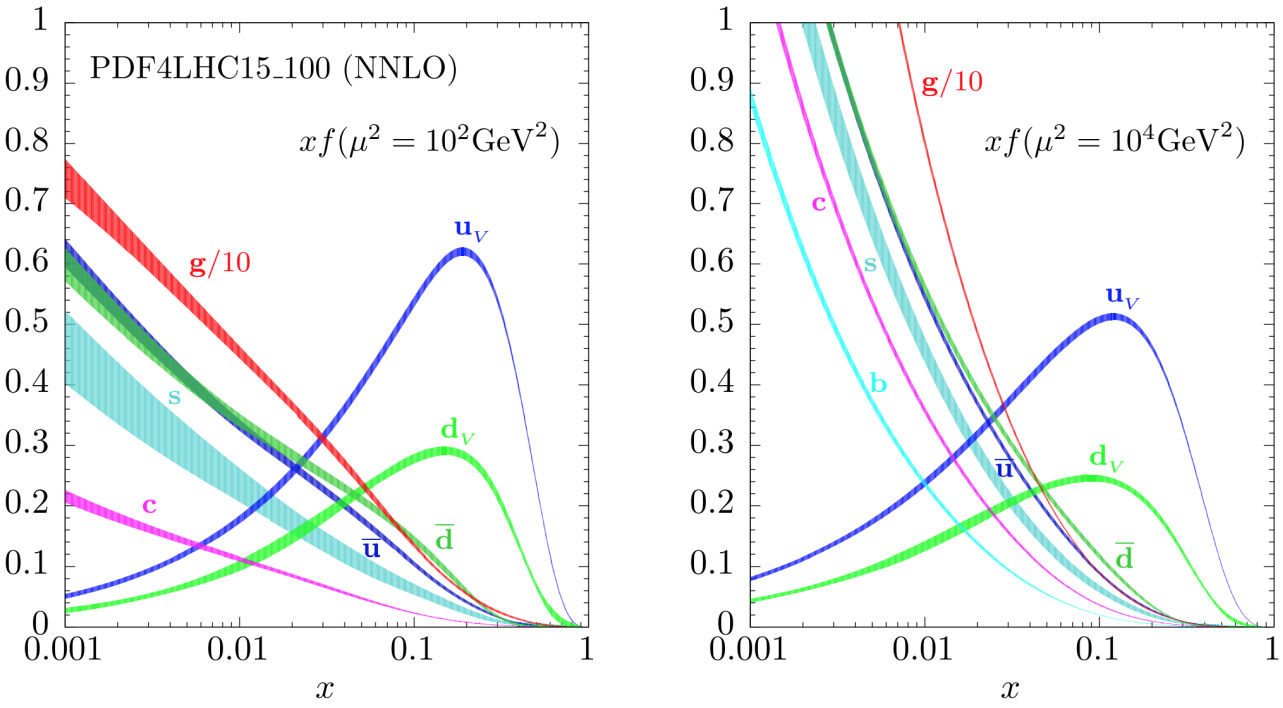

Figure 14: The evolution of a PDF4LHC15 NNLO Hessian set from $Q^2 = 10^2$ GeV to $Q^2 = 10^4$ GeV using the DGLAP. Notice the increase in the sea quark density. The PDFs include one standard deviation uncertainty band.

1.2.2 The Drell-Yan process

The DY process happens during the high-energy hadron-hadron scattering when quark and antiquark annihilate to form an electroweak boson [11]. It is postulated that DY cross-section in a proton-proton scattering $\sigma^{DY}(pp \to l^+l^- + X)$ can be expressed through the cross-sections of the corresponding parton-parton scattering cross-section convoluted with the PDFs of these partons:

$$\frac{d^2\sigma^{DY}}{dydM^2} = \sum_{a,b=q,\bar{q},g} \int_{\tau_1}^{1} dx_1 f_a(x_1,\mu_F^2) \int_{\tau_2}^{1} dx_2 f_b(x_2,\mu_F^2) \frac{d^2\hat{\sigma}_{ab}^{DY}}{dydM^2}(x_1,x_2,y,M^2,\mu_R^2,\mu_F^2). \tag{1.6}$$

In this equation $y = \frac{1}{2}\log\frac{E+p_z}{E-p_z}$ represents rapidity, M^2 is the invariant mass of the lepton pair, μ_F and μ_R are factorization and renormalisation scales correspondingly. Integration limits $\tau_{1,2} = \sqrt{\frac{Q^2}{s}}e^{\pm y}$ with s being the centre-of-mass energy of the two incoming protons. The partonic cross-sections can be in turn computed perturbatively as a series expansion in α_s [2]:

$$\frac{d^2\hat{\sigma}_{ab}^{DY}}{dydM^2}(x_1, x_2, y, M^2, \mu_R^2, \mu_F^2) = \sum_{n=0}^{\infty}\left(\frac{\alpha_s\mu_R^2}{2\pi}\right)^n \frac{d^2\hat{\sigma}_{ab}^{(n)DY}}{dydM^2}. \tag{1.7}$$

The exact sum of the expansion does not depend on the μ_F and μ_R parameters. However, finite-order calculations demand a specific choice for the two parameters. One of the common choices for the DY process is putting $\mu_F = \mu_R = M$, with M being the mass of the dilepton pair.
From equation 1.6 we can see that the rapidity distribution of the vector boson explicitly depends on the PDFs both in terms of flavour decomposition and in the sense of a particular PDF set. Figure 15 demonstrates different rapidity distributions for two centre-of-mass energies and two different PDF sets.

Let us consider partonic cross-sections, which can be constructed using an analogy from QED

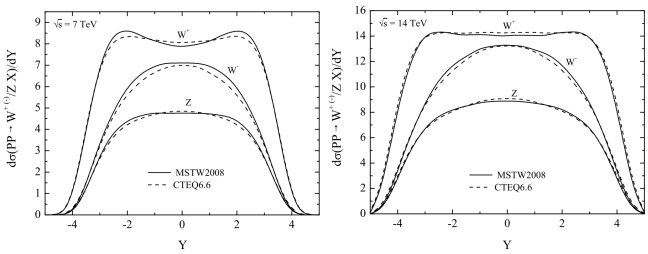

Figure 15: Rapidity distribution for the vector bosons using MSTW2008 and CTEQ6.6 PDF sets for the centre-of-mass energies of 7 and 14 TeV [12].

$e^+e^- \to \mu^+\mu^-$ - a flavour-changing process:

$$\hat{\sigma}(q\bar{q} \to e^+e^-) = \frac{4\pi\alpha_s^2}{3s}\frac{1}{N}Q_q^2. \tag{1.8}$$

Here Q_q^2 is the quark charge, $1/N$ stands for the colour factor and underlines the fact that quark and antiquark must have the matching colour in order to annihilate. In a similar way we can obtain the cross-section of the sub-processes of W and Z bosons production:

$$\begin{aligned}\hat{\sigma}^{q\bar{q}'\to W} &= \tfrac{\pi}{3}\sqrt{2}G_F M_W^2|V_{qq'}|^2\delta(s - M_W^2),\\ \hat{\sigma}^{q\bar{q}'\to Z} &= \tfrac{\pi}{3}\sqrt{2}G_F M_W^2(v_q^2 + a_q^2)\delta(s - M_Z^2),\end{aligned} \tag{1.9}$$

where $V_{qq'}$ is the element of the Cabibbo-Kobayashi-Maskawa (CKM) matrix, v_q (a_q) is a vector (axial vector) that couples the Z boson to the quarks. Figure 17 shows the contributions of different parton flavours into W^+ and W^- cross-sections. An assumption of narrow W resonance was used. The fact that the bosons with opposite charges are formed from different quarks makes a notable difference at the LHC experiments. Figure 16 contains the comparison of the results obtained at the LHC experiments with the NNLO theoretical predictions that use different PDF sets.

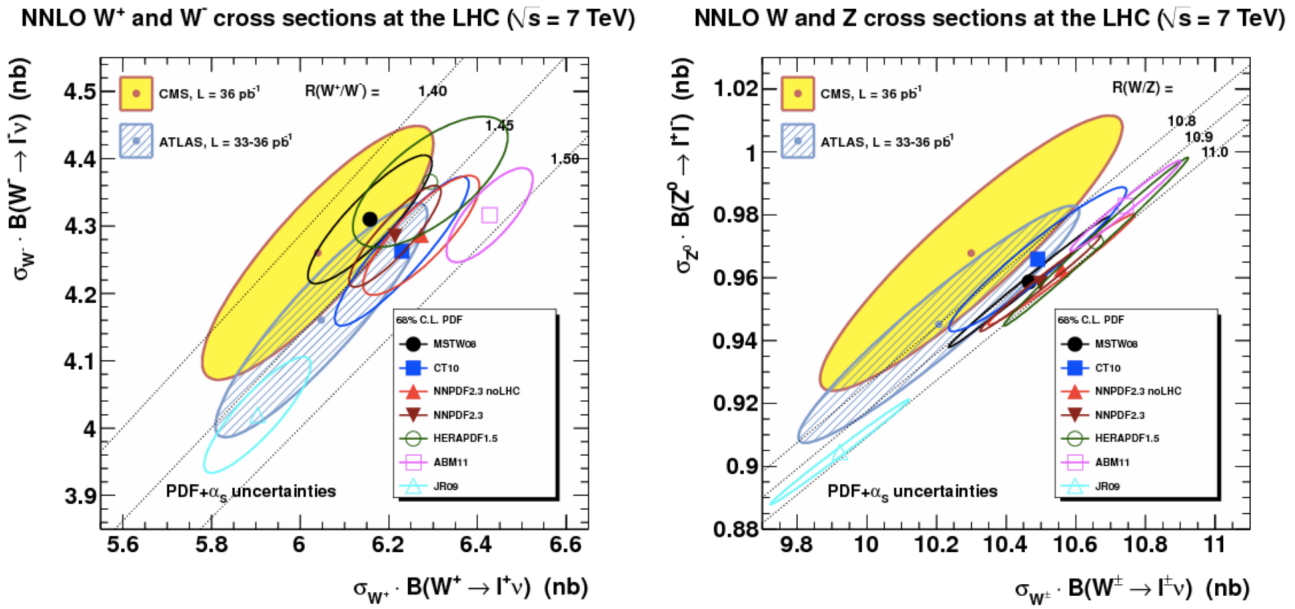

Figure 16: W and Z boson cross sections LHC at 7 TeV. ATLAS and CMS results, compared to NNLO predictions for various PDF sets [13].

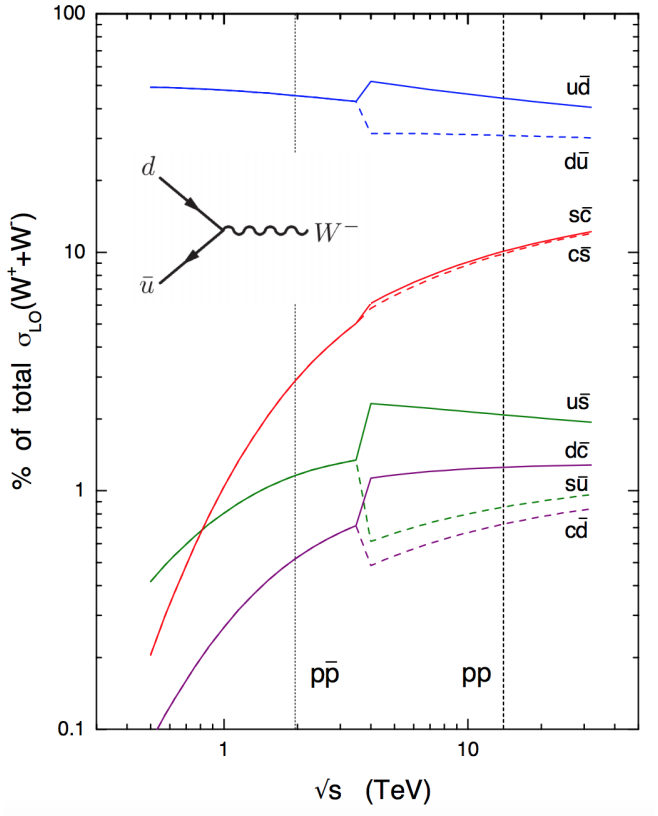

Figure 17: Parton contributions to the cross-sections of W^+ and W^- bosons for LHC and Tevatron cases [14].

1.3 Transverse momentum of massive vector bosons

The leading-order model of the DY process assumes the colliding partons to have their momentum perfectly collinear with the proton as a whole, which would mean that the vector boson p_T should peak at zero. However, most of the massive vector bosons produced in the DY process have a small yet non-zero transverse momentum $p_T \ll M_V$. This occurs due to a non-perturbative effect of partons moving within the colliding protons, having an intrinsic momentum of their own. This intrinsic momentum $< k_T > \backsim \Lambda_{QCD}$ is well parametrized using a Gaussian distribution with average value of 500 [15] or 700 GeV [16], although there are ongoing efforts for a more sophisticated parametrization that would allow a better modelling of the lower part of vector boson p_T spectrum [17].
The spectrum at higher values of p_T is determined by hard perturbative parton emission(s) like $q\bar{q} \to Vg$, $qg \to Vq$. The corresponding amplitudes can be conveniently expressed using Mandelstam variables:

$$\begin{aligned} \sum|\mathcal{M}^{q\bar{q}'\to Wg}|^2 &= \alpha_s\sqrt{2}\pi G_F M_W^2 |V_{q\bar{q}'}|^2 \tfrac{8}{9}\tfrac{t^2+u^2+2M_W^2 s}{tu}, \\ \sum|\mathcal{M}^{qg\to Wq'}|^2 &= \alpha_s\sqrt{2}\pi G_F M_W^2 |V_{q\bar{q}'}|^2 \tfrac{1}{3}\tfrac{s^2+u^2+2M_W^2 t}{-su}, \end{aligned} \tag{1.10}$$

where the summation is performed over colours and spins in the final and initial states. Integrating these partonic matrix elements with the PDFs one can obtain the transverse momentum distribution $d\sigma/dp_T$. Further precision can be obtained by considering corrections from next-to-leading order processes $\backsim O(\alpha_s^2)$ like $q\bar{q} \to Vgg$ - that would mainly affect the high p_T tail of the distribution.
The matrix elements in 1.10 become singular when the emitted partons become soft or collinear to the initial-state partons - it is related to the poles at $u = 0$ and $t = 0$ in the denominator. Also for the NLO processes like $q\bar{q} \to Vgg$ a singularity arises if the two final-state gluons are collinear. This creates a problem for the calculation of the low-p_T part of the spectrum. Mathematically it is reflected in the appearance of different powers of logarithms like $\log M_W^2/p_T^2$ in all orders of cross-section expansion in α_s, which leads to divergences when p_T is small. This forces us to look for alternative approach that would take into account all the orders of the expansion.
All-order resummation may be performed in a variety of approaches, one of the most popular is provided by parton showers. Its numerical implementation is available in a number of Monte-Carlo generators, PYTHIA, HERWIG and SHERPA are among the most used. It appears that for the case of soft and collinear gluon emission it is possible to factorize and exponentiate the logarithms in a *Sudakov form factor*, such that:

$$\begin{aligned} &\tfrac{d\sigma}{dp_T^2} = \sigma\tfrac{d}{dp_T^2}\exp\left\{-\tfrac{\alpha_s C_F}{2\pi}\log^2\tfrac{M_W^2}{p_T^2}\right\}, \\ &\exp\left\{-\tfrac{\alpha_s C_F}{2\pi}\log^2\tfrac{M_W^2}{p_T^2}\right\} = 1 - \tfrac{\alpha_s}{2\pi}C_F\ln^2\tfrac{M_W^2}{p_T^2} + \tfrac{1}{2!}\left(\tfrac{\alpha_s}{2\pi}\right)^2 C_F^2\ln^4\tfrac{M_W^2}{p_T^2} - \tfrac{1}{3!}\left(\tfrac{\alpha_s}{2\pi}\right)^3 C_F^3\ln^6\tfrac{M_W^2}{p_T^2} + \ldots \end{aligned} \tag{1.11}$$

The exponential $\exp\{G(\alpha_s, L)\}$, where $L = \log M_W^2/p_T^2$ is called the Sudakov form-factor. Its expansion by the powers of α_s defines the resummation accuracy: the term $\backsim O(\alpha_s)$ is called the leading logarithm (LL), term with $\backsim O(\alpha_s^2)$ is the next-to-leading logarithm (NLL) and so on.
The cross-sections obtained with the resummation methods provide a good prediction for soft and

collinear emissions at low $p_T \ll M_W$. In order to get a combined cross-section for higher p_T region the resummed cross-section has to be *matched* with the fixed-order cross-sections of the corresponding power in α_s.

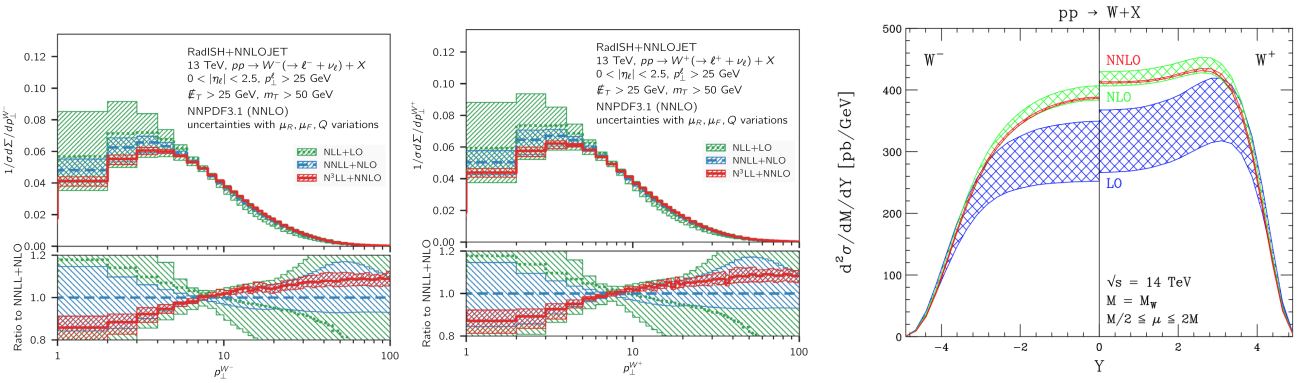

(a) W^- transverse momentum spectrum [18].

(b) W^+ transverse momentum spectrum [18].

(c) $W^\pm$ rapidity distribution [19].

Figure 18: Kinematic distributions for $W^\pm$ with corrections.

Bibliography

[1] M. Awramik et al. "Precise prediction for the W boson mass in the standard model". In: *Phys. Rev. D* 69 (2004), p. 053006. DOI: 10.1103/PhysRevD.69.053006. arXiv: hep-ph/0311148.

[2] Jun Gao, Lucian Harland-Lang, and Juan Rojo. "The Structure of the Proton in the LHC Precision Era". In: *Phys. Rept.* 742 (2018), pp. 1–121. DOI: 10.1016/j.physrep.2018.03.002. arXiv: 1709.04922 [hep-ph].

[3] John C. Collins, Davison E. Soper, and George F. Sterman. "Factorization of Hard Processes in QCD". In: vol. 5. 1989, pp. 1–91. DOI: 10.1142/9789814503266_0001. arXiv: hep-ph/0409313.

[4] J. D. Bjorken. "Asymptotic Sum Rules at Infinite Momentum". In: *Phys. Rev.* 179 (5 Mar. 1969), pp. 1547–1553. DOI: 10.1103/PhysRev.179.1547. URL: https://link.aps.org/doi/10.1103/PhysRev.179.1547.

[5] Richard P. Feynman. "Very High-Energy Collisions of Hadrons". In: *Phys. Rev. Lett.* 23 (24 Dec. 1969), pp. 1415–1417. DOI: 10.1103/PhysRevLett.23.1415. URL: https://link.aps.org/doi/10.1103/PhysRevLett.23.1415.

[6] L.N. Lipatov. "The parton model and perturbation theory". In: *Sov. J. Nucl. Phys.* 20 (1975), pp. 94–102.

[7] G. Altarelli and G. Parisi. "Asymptotic freedom in parton language". In: *Nuclear Physics B* 126.2 (1977), pp. 298–318. ISSN: 0550-3213. DOI: https://doi.org/10.1016/0550-3213(77)90384-4. URL: http://www.sciencedirect.com/science/article/pii/0550321377903844.

[8] V.N. Gribov and L.N. Lipatov. "Deep inelastic e p scattering in perturbation theory". In: *Sov. J. Nucl. Phys.* 15 (1972), pp. 438–450.

[9] Yuri L. Dokshitzer. "Calculation of the Structure Functions for Deep Inelastic Scattering and e+ e- Annihilation by Perturbation Theory in Quantum Chromodynamics." In: *Sov. Phys. JETP* 46 (1977), pp. 641–653.

[10] Max Klein. "Future Deep Inelastic Scattering with the LHeC". In: *From My Vast Repertoire ...: Guido Altarelli's Legacy*. Ed. by Aharon Levy, Stefano Forte, and Giovanni Ridolfi. 2019, pp. 303–347. DOI: 10.1142/9789813238053_0015. arXiv: 1802.04317 [hep-ph].

[11] Sidney D. Drell and Tung-Mow Yan. "Massive Lepton-Pair Production in Hadron-Hadron Collisions at High Energies". In: *Phys. Rev. Lett.* 25 (5 Aug. 1970), pp. 316–320. DOI: 10.1103/PhysRevLett.25.316. URL: https://link.aps.org/doi/10.1103/PhysRevLett.25.316.

[12] Francis Halzen, Yu Seon Jeong, and C.S. Kim. "Charge Asymmetry of Weak Boson Production at the LHC and the Charm Content of the Proton". In: *Phys. Rev. D* 88 (2013), p. 073013. DOI: 10.1103/PhysRevD.88.073013. arXiv: 1304.0322 [hep-ph].

[13] Michelangelo L. Mangano. "Production of electroweak bosons at hadron colliders: theoretical aspects". In: vol. 26. 2016, pp. 231–253. DOI: 10.1142/9789814733519_0013. arXiv: 1512.00220 [hep-ph].

[14] A D Martin et al. "Parton Distributions and the LHC: W and Z Production; rev. version". In: *Eur. Phys. J. C* 14.hep-ph/9907231. DTP-99-64. OUTP-99-31-P. RAL-TR-99-047 (July 1999), 133–145. 30 p. DOI: 10.1007/s100520000324. URL: https://cds.cern.ch/record/392675.

[15] A. Bermudez Martinez et al. "Production of Z bosons in the parton branching method". In: *Phys. Rev. D* 100 (7 Oct. 2019), p. 074027. DOI: 10.1103/PhysRevD.100.074027. URL: https://link.aps.org/doi/10.1103/PhysRevD.100.074027.

[16] R.Keith Ellis, W.James Stirling, and B.R. Webber. *QCD and collider physics*. Vol. 8. Cambridge University Press, Feb. 2011. ISBN: 978-0-511-82328-2, 978-0-521-54589-1.

[17] Francesco Hautmann, Ignazio Scimemi, and Alexey Vladimirov. "Non-perturbative contributions to vector-boson transverse momentum spectra in hadronic collisions". In: *Physics Letters B* 806 (2020), p. 135478. ISSN: 0370-2693. DOI: https://doi.org/10.1016/j.physletb.2020.135478. URL: http://www.sciencedirect.com/science/article/pii/S0370269320302823.

[18] Wojciech Bizon et al. "The transverse momentum spectrum of weak gauge bosons at N ^{3} LL + NNLO". In: *Eur. Phys. J. C* 79.10 (2019), p. 868. DOI: 10.1140/epjc/s10052-019-7324-0. arXiv: 1905.05171 [hep-ph].

[19] Charalampos Anastasiou et al. "High precision QCD at hadron colliders: Electroweak gauge boson rapidity distributions at NNLO". In: *Phys. Rev. D* 69 (2004), p. 094008. DOI: 10.1103/PhysRevD.69.094008. arXiv: hep-ph/0312266.